Title

Highly Efficient Luminescent Metal—Organic Framework for the Simultaneous Detection and Removal of Heavy Metals from Water

Journal

ACS Applied Materials & Interfaces, 8(44)

ISSN

1944-8244

Authors

Rudd, Nathan D

Wang, Hao

Fuentes-Fernandez, Erika MA

et al.

Publication Date

2016-11-09

DOI

10.1021/acsami.6b10890

Peer reviewed

ACS APPLIED MATERIALS & INTERFACES

Research Article

www.acsami.org

Highly Efficient Luminescent Metal–Organic Framework for the Simultaneous Detection and Removal of Heavy Metals from Water

Nathan D. Rudd,[†] Hao Wang,[†] Erika M. A. Fuentes-Fernandez,[‡] Simon J. Teat,[§] Feng Chen,[∥] Gene Hall,[†] Yves J. Chabal,[‡] and Jing Li*[,†]

[†]Department of Chemistry and Chemical Biology, Rutgers University, 610 Taylor Road, Piscataway, New Jersey 08854, United States

[‡]Department of Materials Science and Engineering, University of Texas at Dallas, 800 West Campbell Road, Richardson, Texas 75080, United States

[§]Advanced Light Source, Lawrence Berkeley National Laboratory, 1 Cyclotron Road, Berkeley, California 94720, United States

[∥]Department of Chemistry, Biochemistry and Physics, Rider University, 2083 Lawrenceville Road, Lawrenceville, New Jersey 08648, United States

Supporting Information

ABSTRACT: We have designed and synthesized an isoreticular series of luminescent metal–organic frameworks (LMOFs) by incorporating a strongly emissive molecular fluorophore and functionally diverse colinkers into Zn-based structures. The three-dimensional porous networks of LMOF-261, -262, and -263 represent a unique/new type of nets, classified as a 2-nodal, (4,4)-c net (mot-e type) with 4-fold, class IIIa interpenetration. All compounds crystallize in a body-centered tetragonal crystal system (space group $I4_1/a$). A systematic study has been implemented to analyze their interactions with heavy metals. LMOF-263 exhibits impressive water stability, high porosity, and strong luminescence, making it an excellent candidate as a fluorescent chemical sensor and adsorbent for aqueous contaminants. It is extremely responsive to toxic heavy metals at a parts per billion level (3.3 ppb Hg^{2+}, 19.7 ppb Pb^{2+}) and demonstrates high selectivity for heavy metals over light metals, with detection ratios of 167.4 and 209.5 for Hg^{2+}/Ca^{2+} and Hg^{2+}/Mg^{2+}, respectively. Mixed-metal adsorption experiments also show that LMOF-263 selectively adsorbs Hg^{2+} over other heavy metal ions in addition to light metals. The Pb^{2+} K_{SV} value for LMOF-263 (55,017 M^{-1}) is the highest among LMOFs reported to date, and the Hg^{2+} K_{SV} value is the second highest (459,446 M^{-1}). LMOF-263 exhibits a maximum adsorption capacity of 380 mg Hg^{2+}/g. The Hg^{2+} adsorption process follows pseudo-second-order kinetics, removing 99.1% of the metal within 30 min. An in situ XPS study provides insight to help understand the interaction mechanism between Hg^{2+} and LMOF-263. No other MOFs have demonstrated such a high performance in both the detection and the capture of Hg^{2+} from aqueous solution.

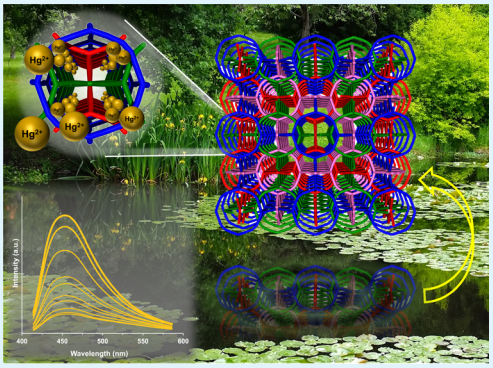

KEYWORDS: *luminescent metal–organic framework, heavy metal detection, heavy metal adsorption, ligand-based emission, isoreticular series*

INTRODUCTION

Effective detection and removal of toxic heavy metals (Hg^{2+}, Pb^{2+}, Cd^{2+}, and so forth) from water sources are paramount to regions spanning the globe. Pollution from mines, factories, or even poorly constructed water supply pipes lead to devastating effects on the environment and vital biological processes, including human health. Recent crises involving drinking water contamination in Flint, Michigan and Newark, New Jersey have proven that these issues do not just exist within developing nations—heavily industrialized areas and cities with antiquated water regulations have a direct and detrimental effect on our drinking water supplies.[1] Alternatively, agricultural communities in under-industrialized areas have high concentrations of heavy metals in groundwater (from assorted agrochemicals, textiles, metallurgy, and so forth).[2] Not only does contaminated groundwater affect drinking supplies, but also these metals also leech into the soil and accumulate in plants and animals. This expands the number of exposed people and ecosystems beyond the agricultural communities.

The ability to detect ultralow levels of toxic metals is of emerging importance. In order to remediate water supplies, it is best to detect toxic metals as early as possible, before the concentrations increase, accumulate in the local environment and cause considerable damage. Previous studies have used a variety of materials that have lowered the threshold for detection. Electrochemical methods[3−6] for the detection of mercury have vastly lowered sensing limits, however these methods are expensive, cumbersome, and require higher

Received: August 29, 2016
Accepted: October 13, 2016
Published: October 13, 2016

DOI: 10.1021/acsami.6b10890
ACS Appl. Mater. Interfaces 2016, 8, 30294−30303

technical prowess. Techniques that measure sample absorbance to detect trace mercury levels[7,8] have allowed for more portable instrumentation, but it has been shown that fluorescence based sensors have lower detection limits.[9]

The possibility of synthesizing new fluorescent materials that selectively bind heavy metals has drawn further attention.[10−12] Luminescent metal−organic frameworks (LMOFs) have recently been developed as chemical sensors due to their high porosity, tunability, and mild synthetic conditions.[13−22] Most of the previous studies making use of LMOFs for heavy metal detection have focused on functionalized prototype materials to increase selectivity for toxic metal ions or to enhance luminescence, without addressing their capture/removal potential from aqueous solution.[23−30] Other studies have centered on tailoring MOFs to boost their uptake capacity for heavy metal ions, without providing fluorescence-based quantitative detection ability for these contaminants.[31−33] Obtaining a material that can simultaneously detect and remove heavy metals from water would greatly enhance the water remediation process, although research that places a spotlight on both functionalities is sparse.[33,34]

Effective fluorescence detection and adsorption of heavy metals relies on both selectivity and sensitivity—namely the signal responses must be sensitive to the change in concentration and interactions should be analyte specific.[33,35,36] Dual-ligand MOFs that offer both luminescence and targeted functionality provide a unique scaffold that can echo these important properties.[37,38]

Following these guidelines, we have recently developed a new strategy to design highly porous LMOFs for possible use as dual-functional fluorescence sensors and adsorbents.[39−41] By incorporation of a chromophore-based ligand along with a structure-modulating coligand,[42] we have succeeded in synthesizing a number of LMOFs with high stability, specified porosity, surface functionality, targeted emission energy, and strong luminescence. For example, the combination of a green-emitting chromophore and a tricarboxylate coligand leads to LMOF-251 with desired yellow emission and significantly enhanced fluorescence quantum yield.[39]

The aforementioned characteristics make these LMOFs promising candidates for selective detection and effective capture of heavy metals. In this study, we report the design and synthesis of a series of isoreticular LMOFs[43] built on a tetradentate chromophore and a dicarboxylate-based coligand with varying functional moieties and a detailed study of their heavy metal detection and uptake potential. We show that the LMOF with thio-functionalization exhibits extremely sensitive and selective optical detection of heavy metals over non-hazardous lighter metals, as well as high performance in the removal of heavy metals from aqueous solution.

EXPERIMENTAL SECTION

General Information. All reagents are used as purchased unless specified otherwise. Detailed information on the sources of chemicals is in the Supporting Information (SI).

Synthesis of Chromophore Ligand. 1,1,2,2-tetraphenylethene (tpe, **A**) powder was reacted with liquid bromine to produce 1,1,2,2-tetrakis(4-bromophenyl)ethene (Br_4-tpe, **B**) and further purified via recrystallization in methylene chloride/methanol, as shown in Scheme 1. To attach the pyridine moiety to the tetradentate segment, a Suzuki coupling was carried out between Br_4-tpe and pyridine-4-boronic acid, catalyzed by palladium(II) acetate.

Scheme 1. tppe Synthesis

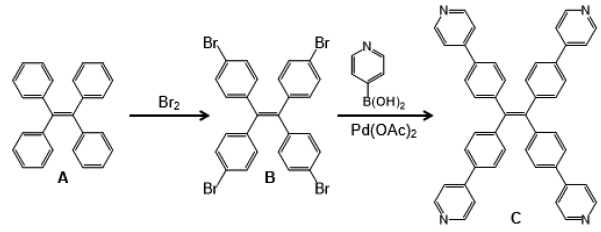

The fluorophore 1,1,2,2-tetrakis(4-(pyridine-4-yl)phenyl)ethane (4-tppe, **C**) product was synthesized according to literature procedures.[39] Product yield was 75%.

Synthesis of H_2hfdc. The linker H_2hfdc (**E**) was synthesized through use of the Huang Modification.[37] H_2ofdc [9-oxo-9*H*-fluorene-2,7-dicarboxylic acid] (**D**) (3 g, 11.2 mmol) and NaOH (2.64 g, 6 equiv) were mixed with hydrazine monohydrate (2.25 mL, 16 equiv) and ethylene glycol (100 mL) for 12 h at reflux (Scheme 2). Hydrazine

Scheme 2. H_2hfdc Synthesis

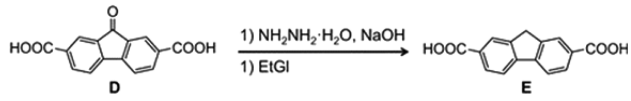

monohydrate was evaporated from the mixture and the temperature raised to keep the ethylene glycol at reflux. After the reaction ceased, the solution was neutralized using excess water, and the pH was slowly decreased to ∼1 using aliquots of concentrated HCl. The orange solid (2.5 g, 86% yield) was filtered and washed with excess water.

Synthesis of H_2dbtdcO_2. The sulfone-functionalized ligand H_2dbtdcO_2 [**G**, dibenzo[*b*,*d*]thiophene-3,7-dicarboxylic acid-5,5-dioxide} was synthesized according to the work of Olkhovik et al.[44] As Scheme 3 shows, dimethyl biphenyl-4,4′-dicarboxylate (**F**, 5 g, 18.5

Scheme 3. H_2dbtdcO_2 Synthesis

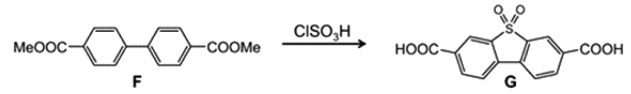

mmol) was dissolved in chlorosulfonic acid (21.57 g, 10 equiv). The mixture was heated at reflux for 3 h, or until no more HCl was produced as a byproduct. At this time, the mixture was poured onto crushed ice to quench the reaction. White solid was separated via vacuum filtration, washed with water, and dried to produce H_2dbtdcO_2 (4.5 g, 80% yield).

Synthesis of Zn_2(ofdc)$_2$(tppe) (LMOF-261). Solvothermal reactions of $Zn(NO_3)_2{\cdot}6H_2O$ (0.030 g, 0.1 mmol), tppe (0.024 g, 0.4 mmol), and ofdc (0.0134g, 0.05 mmol) in a mixed solvent system (DMA:iPrOH:DMSO, 4:1:1) were prepared in 20 mL glass vials. The reaction mixture initially was kept under sonication until all solids were dissolved, then the vials were kept at 150 °C for 24 h. After the reaction mixture was cooled to room temperature, the yellow needle-shaped crystals were collected via vacuum filtration and washed with DMA.

Synthesis of Zn_2(hfdc)$_2$(tppe) (LMOF-262). Solvothermal reactions of $Zn(NO_3)_2{\cdot}6H_2O$ (0.015 g, 0.05 mmol), tppe (0.019 g, 0.3 mmol), and hfdc [9*H*-fluorene-2,7-dicarboxylic acid] (0.025 g, 0.1 mmol) were prepared similarly to LMOF-261 reactions, instead reacting at 120 °C for 3 d. Orange rod crystals were filtered after the reaction was brought to room temperature and washed with DMA.

Synthesis of Zn_2(dbtdcO_2)$_2$(tppe) (LMOF-263). Solvothermal reactions of $Zn(NO_3)_2{\cdot}6H_2O$ (0.030 g, 0.1 mmol), tppe (0.024 g, 0.4 mmol), and H_2dbtdcO_2 [dibenzo[*b*,*d*]thiophene-3,7-dicarboxylic acid 5,5-dioxide] (0.030 g, 0.1 mmol) were prepared similarly to LMOF-261 reactions. After the reaction mixture was cooled to room

DOI: 10.1021/acsami.6b10890
ACS Appl. Mater. Interfaces 2016, 8, 30294−30303

temperature, pale yellow needle-shaped crystals were collected via vacuum filtration and washed with DMA.

Structural Analysis of LMOF-261. Single crystal X-ray diffraction data for LMOF-261 were collected on a Bruker D8 diffractometer with PHOTON 100 detector using the synchrotron source (λ = 0.7749 Å) at the Advanced Light Source 11.3.1 Chemical Crystallography beamline (Table 1). All non-hydrogen atoms were refined anisotropically; hydrogen atoms were placed geometrically, constrained, and refined with a riding model. The unresolvable electron density from the void space in the structure was removed by SQUEEZE.

Table 1. Single Crystal Data of LMOF-261

compound	LMOF-261
formula	$C_{38}H_{22}N_2O_5Zn$
M	651.94
crystal system	tetragonal
space group	$I4_1/a$
a (Å)	33.9529(14)
b (Å)	33.9529(14)
c (Å)	17.1833(8)
α/deg	90
β/deg	90
γ/deg	90
V (Å^3)	19808.9(19)
Z	16
temperature (K)	100(2)
λ (radiation wavelength) (Å)	0.7749
D (g/cm^3)	0.874
reflections collected	126056
$R1^a$ [$I > 2\sigma(I)$]	0.0585
$wR2^b$ [$I > 2\sigma(I)$]	0.1516
goodness-of-fit	1.066
CCDC no.	1478942

$^a R1 = \sum|F_o - F_c|/\sum|F_o|$ $^b wR2 = \sum[w(F_o^2 - F_c^2)^2]/w(F_o^2)^2]^{1/2}$

The powder X-ray diffraction (PXRD) patterns were collected on a Rigaku Ultima-IV diffractometer using monochromatic Cu K_α radiation (λ = 1.5406 Å). Data were collected between 3 and 45° 2θ with step size 0.02° and scanning rate 2.0°/min.

Fluorescence Titration. Stock solutions of M^{2+} (M: Hg^{2+}, Pb^{2+}, Ca^{2+} and Mg^{2+}) were prepared by dissolving MCl_2 salts into ultrapure, deionized water. An as-made sample of LMOF-263 was placed into water (0.25 g/L) and gently sonicated. LMOF-263 was easily suspended in water. Photoluminescence (PL) titrations were carried out by incrementally adding aliquots of M^{2+} stock solutions to the LMOF-263 suspension and kept under continuous stirring. The fluorescence spectra were recorded 5 min after adding the appropriate amount of M^{2+} stock solution. This exposure time ensured that analyte entered the LMOF pores. Each measurement was repeated three times, and the average value was used.

RESULTS AND DISCUSSION

Synthesis of an Isoreticular LMOF Series. An isoreticular LMOF series has been synthesized using the tetradentate tppe ligand and several functionalized dicarboxylate linkers as coligands. The formation of a group of LMOFs with the same structure and topology using such coligands would allow us to study, compare, and understand the difference in their sensing behavior in a direct and systematic manner. Crystals of LMOF-261 were obtained through procedures reported above.

Crystal Structure Analysis. LMOF-261 or $[Zn_2(ofdc)_2(tppe)]\cdot S$ (S = solvent guest molecules) crystallizes in the tetragonal crystal system with space group $I4_1/a$. Each Zn^{2+} has distorted tetrahedral coordination to two carboxylate groups from ofdc linkers and two pyridine groups from tppe ligands, forming the PBU (Figure 1a). Each PBU is connected to three other PBUs through ofdc linkers to create a distorted square, with four Zn^{2+} in the same plane (Figure 1b). This distorted square is further connected by tppe ligands to expand the framework in three dimensions. Viewed down the b-axis, an individual net of LMOF-261 exhibits 1D, edge sharing pentagonal and rhombohedral channels (Figure 1b). Along the c-axis, there are two types of 1D channels having square and octagon shaped cross sections, respectively. (Figure 1c). The tetrahedral channels have an aperture of ∼1.7 nm, while the octahedral channels have an aperture of ∼3.7 nm. These channels proliferate down the c-axis, with carbonyl groups pointed directly into the LMOF channels.

The overall structure of LMOF-261 involves a 4-fold interpenetrated framework containing four of these identical nets (Figure 1d). When tppe and ofdc are simplified as 4-c nodes, the structure would be a 2-nodal, (4,4)-c net (mot-e type) with 4-fold, class IIIa interpenetration. This is a unique net type, according to the ToposPro Database. The interpenetrated structure encloses two types of 1D channels down the c-axis: one having a pentagon-shaped cross section (8.1 Å aperture) and the other, with a narrower tetragon-shaped aperture 7.2 Å in diameter.

The simulated pattern from single crystal X-ray diffraction (SCXRD) on LMOF-261 matched the PXRD patterns of LMOF-262 and -263 samples (Figure 2), confirming their structures are isoreticular with respect to the parent LMOF-261.

Pore Characterization. Gas sorption isotherms of LMOF-261 and -263 were collected on a Quantachrome Instruments Autosorb-1 MP volumetric gas sorption analyzer using ultra high purity N_2 (99.999%). Liquid nitrogen was the coolant used to reach cryogenic temperature (77 K). As-made samples of LMOF-261 and -263 were outgassed at 120 °C for 8 h, and the subsequent degassed samples were used. The N_2 isotherm was collected in a pressure range from 10^{-7} to 1 atm at 77 K. Surface area was analyzed using Autosorb V1.50 software. The Brunauer−Emmett−Teller (BET) surface area of LMOF-261 and −263 were 977 and 1004 m^2/g, respectively.

Optical Properties of LMOF-261, -262, and -263. The optical diffuse reflectance spectra of the tppe ligand and the isoreticular series of LMOFs were collected using a Shimadzu UV-3600 spectrophotometer, after which transformation to the Kubelka−Munk function allowed their optical band gaps to be estimated. The HOMO−LUMO energy gaps of tppe, LMOF-261, -262, and -263 are estimated to be 2.3, 2.55, 2.65, and 2.7 eV, respectively (Figure S4).

Photoluminescence (PL) excitation and emission spectra were collected for samples of the LMOF series at room temperature. The ligand tppe showed strong green emission when excited by UV light (λ_{ex} = 365 nm) with an emission maximum at 500 nm.[9] The emissions of all three LMOFs are ligand based, with a maximum of intensity at 514, 516, and 464 nm, for LMOF-261, -262, and -263, respectively (Figure 3). After outgassing these materials for 8 h at 120 °C, the emission energies red-shifted considerably, as seen in (Figure S5). A Hamamatsu C9220-03 spectrophotometer with integrating sphere was used to determine internal quantum yield (IQY) of LMOF-261, -262, and -263 at λ_{ex} = 360 nm (Table S1).

A comparison among three isoreticular counterparts indicated that LMOF-263 has the highest chemical stability as well as fluorescence quantum yield (Table S1). In addition, the

DOI: 10.1021/acsami.6b10890
ACS Appl. Mater. Interfaces 2016, 8, 30294−30303

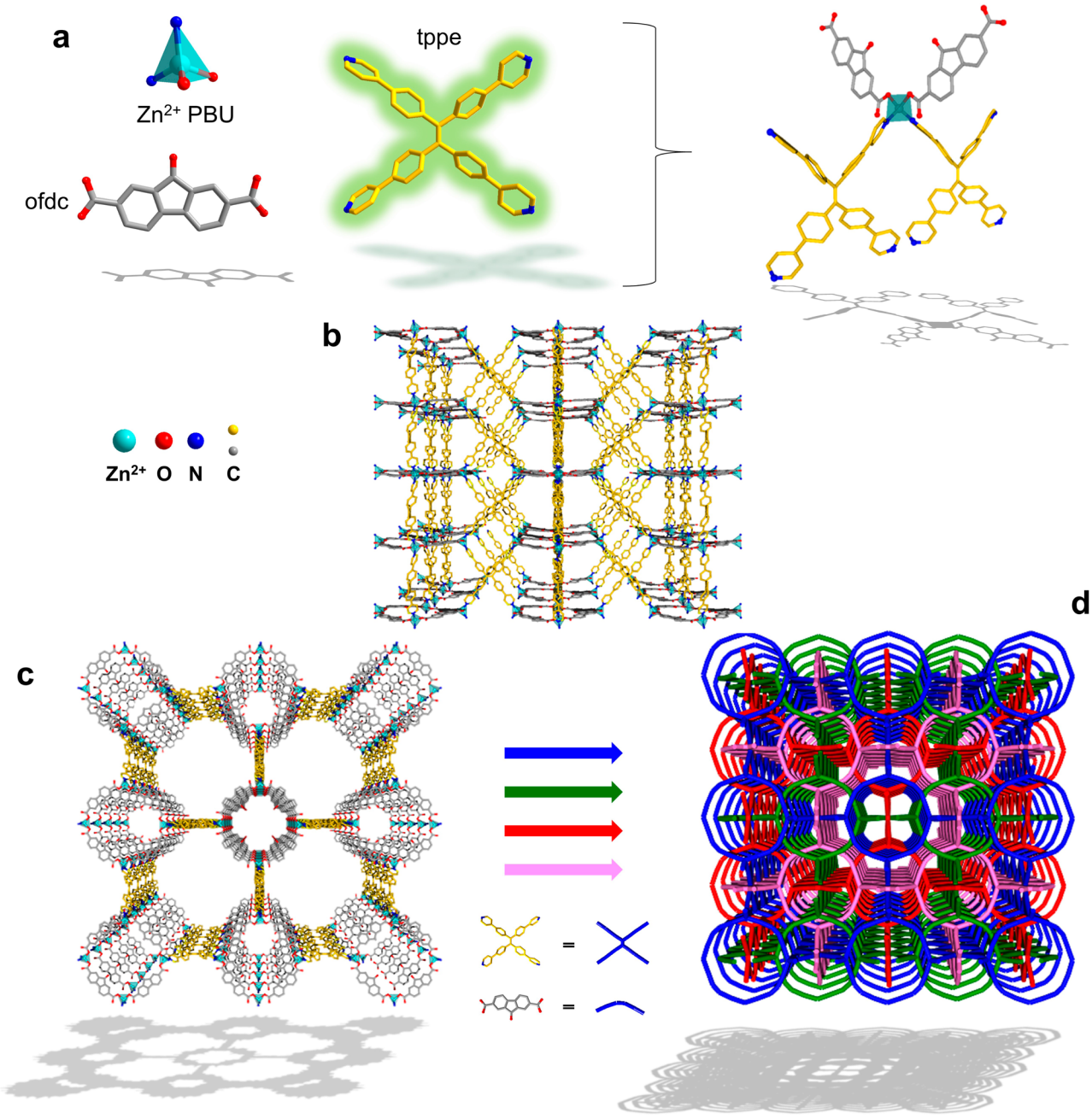

Figure 1. (a) The PBU of LMOF-261, depicting a pseudotetrahedrally coordinated Zn center bound to two fluorophoric tppe ligands and two ofdc linkers. (b) An individual net of the LMOF-261 framework viewed along the *b*-axis, containing 1D, edge sharing pentagonal and rhombohedral channels. (c) The same net depicted down the *c*-axis, showcasing edge sharing octahedral and cylindrical channels. The ofdc linkers point directly into the cylindrical channels extending down the *c*-axis. (d) Simplified LMOF-261 depicting 4-fold interpenetration. Each of the three other nets occupies one octahedral pore of the fourth net to create narrow pentagonal channels, sharing edges from multiple nets.

sulfone functional group on the coligand, clearly detected by FTIR (Section S8), is likely to enhance the interactions between heavy metal ions and LMOF sensor, and therefore, was chosen as the target system for the subsequent sensing experiments.

Heavy Metal Detection. Heavy metals have been identified as serious water contaminants that lead to the dysfunction of vital biological processes. Simple and highly efficient probes that can be used for on-site measurements are vital to monitor low concentrations of heavy metals in water. However, light metals, such as Ca^{2+} or Mg^{2+}, are commonly found in drinking water supplies and provide important functions in biological processes. Therefore, selectivity for toxic metals over these harmless elements would be an important criterion for fluorescent detectors.

Detection of various metal ions (Hg^{2+}, Pb^{2+}, Ca^{2+}, Mg^{2+}) was accomplished by observing the change in PL signal of an aqueous LMOF-263 suspension before and after addition of the analyte. Figure 4a shows the LMOF-263 emission wavelength (λ_{em} = 464 nm, λ_{ex} = 365 nm) stays the same in the solid-state or as a suspension in water, yet the intensity is decreased when suspended in water. LMOF-263 was stable in water for 14 days and stable in pH 4–10 for up to 15 h (Figure S2). The emission intensity at 464 nm (λ_{ex} = 365 nm) decreased when

DOI: 10.1021/acsami.6b10890
ACS Appl. Mater. Interfaces 2016, 8, 30294–30303

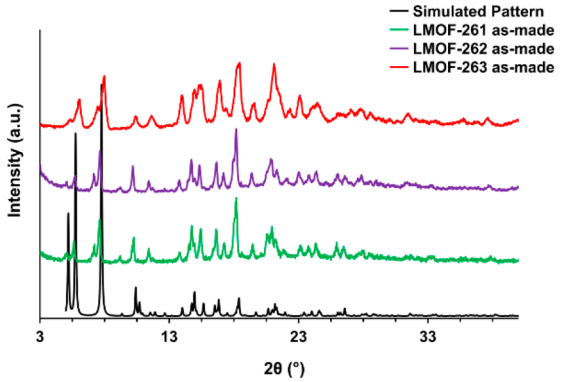

Figure 2. PXRD patterns of the LMOF isoreticular series (LMOF-261, -262, and -263).

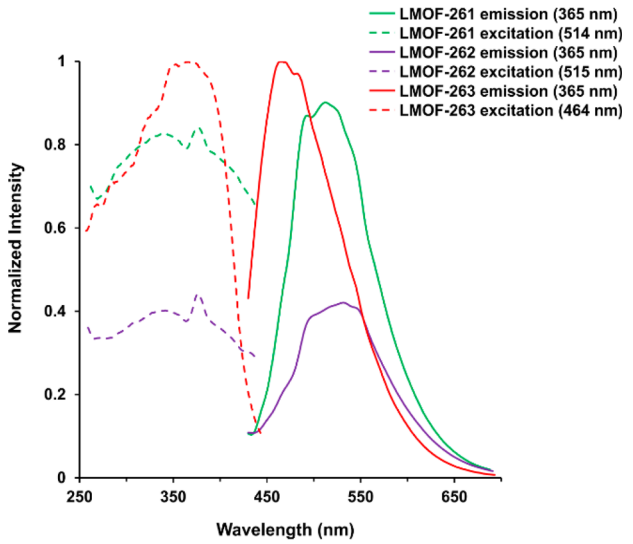

Figure 3. Optical emission (solid) and excitation (dotted) spectra of LMOF-261, -262, and -263.

immersed in water, however that intensity was maintained 15 h after the initial immersion (Figure 4a). While Hg^{2+} detection could be plagued by formation of nonuniform suspensions,[45] LMOF-263 forms a uniform suspension in water, promoting its ease as an on-site detection material.

Upon addition of M^{2+} solution aliquots, the emission intensity of LMOF-263 was quenched to varying degrees, depending on the M^{2+} analyte and concentration. Approximately 84% of the total intensity of LMOF-263 was quenched upon addition of only 19.6 μM of Hg^{2+} (Figure 4b), while 64% of the total intensity was quenched when exposed to 19.6 μM of Pb^{2+} (Figure 4c). The quenching efficiency was quantified using the Stern–Volmer (SV) equation:

$$I_0/I = K_{SV}[Q] + 1$$

where I_0 is the initial emission peak intensity (pre-exposure to analyte), I is the emission peak intensity after addition of analyte, $[Q]$ is the molar concentration of the analyte (or quencher), and K_{SV} is the Stern–Volmer constant, which can be used to quantitatively measure the performance of LMOF-263 as a sensor for heavy metals (Hg^{2+} and Pb^{2+}). As shown in the inset of Figure 4d, at low concentrations, the value I_0/I is directly proportional to metal ion concentration. The K_{SV} was determined to be 459 446 and 55 017 M^{-1} for Hg^{2+} and Pb^{2+}, respectively (Figure S21). The detection limit for Hg^{2+} was determined to be 3.3 and 19.7 ppb for Pb^{2+}. The Hg^{2+} detection limit of LMOF-263 is on par with all photoluminescent MOFs that have been investigated for heavy metal fluorescence detection and exhibits the second highest MOF K_{SV} value reported to date.[23,24,27,29,46−49] The only MOF to exhibit a higher quenching efficiency for Hg^{2+} was the heavily studied PCN-224, for which uptake capacity was not reported.[50] Certain nanomaterials have also demonstrated higher Hg^{2+} K_{SV} values than LMOF-263, however they have no reported adsorption capacity for heavy metals, limiting their use for water remediation efforts.[51,52] The Pb^{2+} fluorescence detection limit and K_{SV} value exceed the performance of any other luminescent MOF.[26,53,54]

In addition to its high sensitivity toward heavy metals, LMOF-263 also exhibits excellent selectivity. On the basis of the Stern–Volmer plots shown in Figure 4d, the K_{SV} values for Ca^{2+} and Mg^{2+} were calculated to be 2745 and 2193 M^{-1}, respectively, which correspond to a detection ratio of 167.4 and 209.5 for Hg^{2+}/Ca^{2+} and Hg^{2+}/Mg^{2+}, respectively. These values clearly indicate that LMOF-263 acts as a highly selective detector for heavy metals only.

Heavy Metal Removal. Materials with high performances for both detection and capture of toxic/hazardous species are rare. Similar to detection requirements, selectivity for heavy metals over light metals is important when removing these contaminants from water. To assess the heavy metal removal performance of LMOF-263, as-made samples (5, 10, and 15 mg; 0.20, 0.41, and 0.62 mM, respectively) were placed in dilute aqueous solutions (35 mL) of $HgCl_2$, $PbCl_2$, $CdCl_2$, $CaCl_2$, and $MgCl_2$ (concentration of M^{2+}, 10 ppm; ~0.350 mg of M^{2+}). After these mixtures were stirred at room temperature for 12 h, the solutions were filtered from the adsorbent and the residual M^{2+} concentrations were determined via ICP-OES, using a Spectro Arcos analyzer with standards from VHG Laboratories (#SM45-500 and SM70B-500). Displayed in Figure 5, LMOF-263 lowers the concentration of Hg^{2+} from 10 ppm to 36 ppb—the adsorbent effectively removes ~99.6% of Hg^{2+} from solution), which is among the highest performances for MOFs.[33]

LMOF-263 (15 mg, 0.62 mM), when exposed to 35 mL solutions of 10 ppm M^{2+} (~0.350 mg M^{2+}), lowers the concentration of Pb^{2+}, Cd^{2+}, Ca^{2+}, and Mg^{2+} to 1.96, 6.60, 10.03, and 7.34 ppm, respectively. LMOF-263 exhibits distinct selectivity toward heavier metals (Hg^{2+}, Pb^{2+}) over lighter metals (Ca^{2+}, Mg^{2+}), as highlighted in Figure 5. Even with an increased amount of adsorbent, the concentrations of Ca^{2+} and Mg^{2+} in the postexposure solutions did not significantly decrease. This is consistent with the detection results shown above.

To further evaluate the selectivity of LMOF-263 for heavy metals over light metals, we carried out adsorption experiments using mixed-metal solutions. Solutions of 10 ppm of Hg^{2+}, Pb^{2+}, Ca^{2+}, and Mg^{2+} (35 mL, ~0.350 mg of each M^{2+}) were prepared and exposed to 10 and 15 mg amounts of LMOF-263 for 15 h (0.41 and 0.62 mM LMOF-263, respectively). Similar amounts of LMOF-263 were also exposed to solutions of 10 ppm of Hg^{2+} as a control and solutions of 10 ppm of Hg^{2+}, Ca^{2+} and Mg^{2+} to investigate the interference of Pb^{2+} ions. Figure 6 displays the LMOF-263 adsorption performance under these competitive conditions. When all four heavy and light metals are mixed, LMOF-263 clearly shows preference toward Hg^{2+} adsorption—approximately 99.2% of the initial amount of Hg^{2+} was removed, lowering the concentration of Hg^{2+} from 10 ppm

DOI: 10.1021/acsami.6b10890
ACS Appl. Mater. Interfaces 2016, 8, 30294−30303

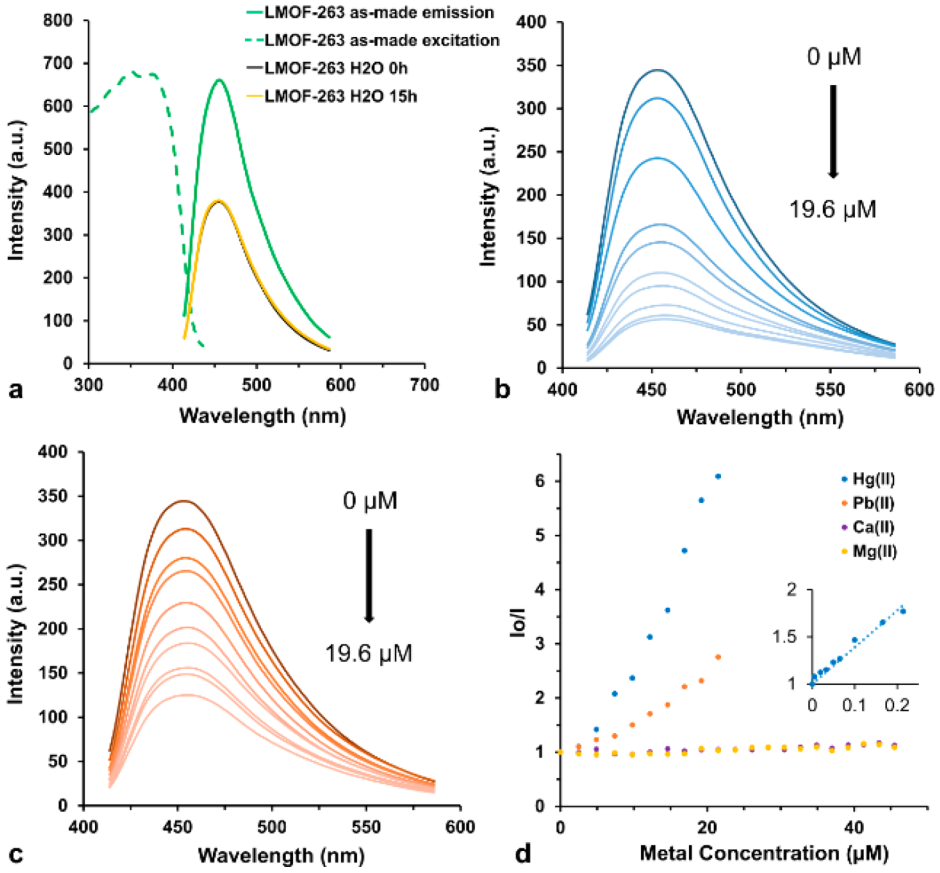

Figure 4. (a) LMOF-263 optical emission in the solid-state and as a suspension in water (0.25 g/L). (b) Emission spectra of LMOF-263 after incremental additions of an aqueous Hg^{2+} solution and (c) Pb^{2+} solution. (d) Stern−Volmer curves (λ_{ex} = 365 nm) for heavy and light metal ions, monitoring LMOF-263 selectivity (inset, Hg^{2+} detection at low concentrations). See Section S11 for average standard deviations of I_0/I values in Hg^{2+} and Pb^{2+} detection trials.

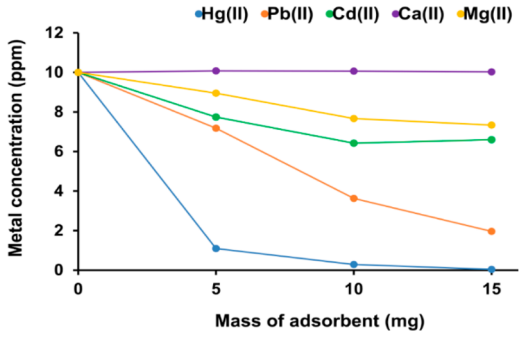

Figure 5. Metal ion concentrations after exposure to 5, 10, or 15 mg of LMOF-263 in 35 mL solutions.

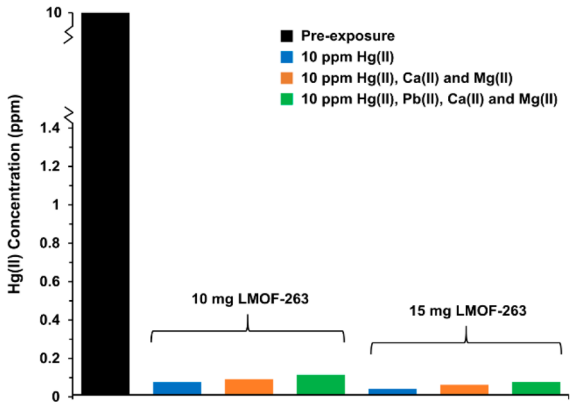

Figure 6. Remaining Hg^{2+} concentrations after exposure to various amounts of LMOF-263 in mixed metal solutions (initial concentrations: 10 ppm M^{2+}, as specified in the legend).

to 78 ppb (Figure 6, 15 mg LMOF-263). When the same amount of adsorbent was exposed to 10 ppm of Hg^{2+} (single-metal solution), 99.6% of the initial Hg^{2+} amount was extracted, lowering the solution Hg^{2+} concentration to 41 ppb. These results provide strong evidence that LMOF-263 selectively interacts with and captures Hg^{2+} over light metals.

To emphasize its practical use as an on-site remediation material, LMOF-263 adsorption kinetics were analyzed. LMOF-263 (15 mg, 0.62 mM) was exposed to solutions of 10 ppm of Hg^{2+} (35 mL) for specific time intervals. As shown in Figure S9, LMOF-263 displays fast pseudo-second-order adsorption kinetics[31,35] (adsorption rate constant: 0.295 g mg^{-1} min^{-1}), with 99.1% of Hg^{2+} removed from solution within 30 min.

Recyclability of an adsorbent is a highly desirable feature for environmental remediation. After the initial exposure to 10 ppm of Hg^{2+} solutions, two additional cycles were carried out on the same MOF sample. The luminescence was fully recovered after each desorption, as determined through PL quenching/enhancement (Figure S6a). The structure of LMOF-263 was well maintained during these cycles (Figure

DOI: 10.1021/acsami.6b10890
ACS Appl. Mater. Interfaces 2016, 8, 30294−30303

S6b) but began to show signs of degradation after that, indicating its limited water stability.

One measure of a sorbent's affinity for some target metal ion is the distribution coefficient (K_d), defined as follows:[55]

$$K_d = [(C_i - C_f)/C_f] \times (V/m)$$

where C_i is the initial metal concentration, C_f is the final equilibrium metal ion concentration, V is the volume of treated solution (mL), and m is the mass of sorbent used (g). K_d values of 1.0×10^5 mL g^{-1} are usually considered to have excellent performance.[56] The K_d value for LMOF-263 on Hg^{2+} in this analysis was determined to be 6.45×10^5 mL g^{-1}. This is on the same order of magnitude as other high performance materials, including Zr-DMBD (9.99×10^5 mL g^{-1}),[33] sulfur-functionalized mesoporous carbon ($6.34–6.82 \times 10^5$ mL g^{-1})[56] and commercial resins (10^4~5.10×10^5 mL g^{-1}).[57]

As further confirmation of mercury uptake into LMOF-263, X-ray fluorescence spectroscopy (XRF) was employed to determine the amount of Hg^{2+} left in filtered LMOF samples after Hg^{2+} exposure. Approximately 15 mg of LMOF-263 was immersed in 35 mL water solutions of various concentrations of Hg^{2+} (10 through 30 000 ppm) for 36 h. After filtration and washing with copious amounts of water, XRF analysis was used to determine the relative weight ratios of Zn^{2+} and Hg^{2+} in the samples (Table S3). The structure of LMOF-263 was stable after exposure to Hg^{2+} for 36 h (Figure S10). Figure 7 displays

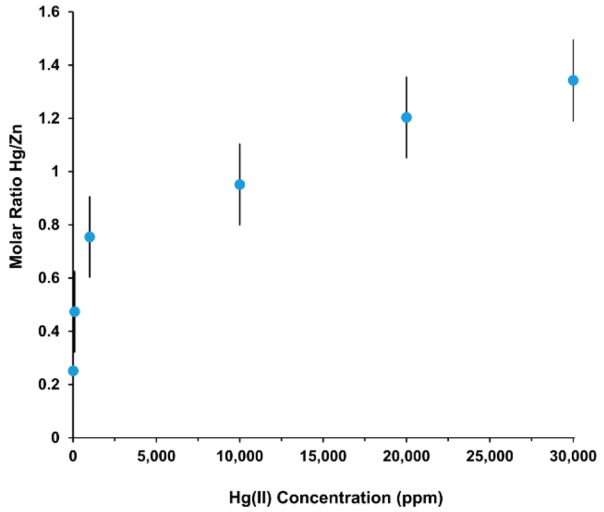

Figure 7. Molar ratio of Hg/Zn (blue dots) in LMOF-263 samples after exposure to 10, 100, 1000, 10 000, 20 000, and 30 000 ppm of Hg^{2+} solutions. These values represent averages over three trials. The error bars represent the average standard deviation of the molar ratio (±0.152 Hg/Zn) over all concentrations.

the molar ratios of Hg^{2+} to Zn^{2+} for samples treated at varied concentrations. After exposure to higher concentrations of Hg^{2+}, the relative weight ratio of Hg^{2+} to Zn^{2+} approaches ~80% and ~20%, respectively, corresponding to approximately 1.3 Hg^{2+} ions per Zn^{2+} ion.

For each unit cell of LMOF-263, there are equimolar amounts of Zn^{2+} and sulfone groups ($[Zn_2(dbtdcO_2)_2tppe]$, from SCXRD analysis on LMOF-261 described above), so there are also 1.3 Hg^{2+} per sulfone moiety. Previous work has demonstrated similar metal analyte interactions with sulfur (>1 metal ion per sulfur atom).[58] From the XRF data, LMOF-263 exhibits an estimated maximum uptake capacity of ~380 mg Hg^{2+}/g, which is at the similar scale compared with the best-performing MOFs for Hg^{2+} adsorption, although in all other cases no quantitative data were provided on their selectivity or sensitivity of fluorescent detection.[33,59–67] While unsaturated metal nodes in HKUST-1 or ligands within UiO-66 have been functionalized with thiol groups to enhance Hg^{2+} uptake (714 and 769 mg Hg^{2+}/g, respectively), these MOFs were reported to have no fluorescence, thus negligible detection potential.[31,32] LMOF-263 displays both a low detection limit and a high uptake performance, establishing itself as an ideal, dual-functional material for water purification applications.

Hg^{2+} Interactions. Details about the microscopic interaction of Hg^{2+} within LMOF-263 can be derived from XPS measurements through analyses of the core level shifts, as detailed in the SI (Section S9). Specifically, the binding energies of C, O, and S were monitored as a function of Hg^{2+} loading. The data show a small (~0.3–0.4 eV) but clear shift of the S core level, and an enhancement of a secondary oxygen peak as the Hg^{2+} concentration increases (Figure S12–S17, Table S4–S5, and Figure S19), and no observed shift of the C core level. When LMOF-263 was exposed to 20 000 ppm Mg^{2+}, there was no shift in the sulfur core level or any enhancement of a secondary oxygen peak (Figure S18). This observation points to a selective interaction of LMOF-263 with heavy metals compared to light metals. These findings are similar to previous studies of Hg^{2+} incorporation in materials (typical XPS binding energy shifts upon Hg^{2+} exposure).[45,47]

Although oxygen and sulfur have similar binding energies with mercury (100.7 and 101 eV, respectively), the sulfur atom within the sulfone group has no lone pairs to interact directly with Hg^{2+}, which also limits the sulfur atom from forming hydrogen bonds in an aqueous environment.[68] Instead, the sulfur atom forms weak π-bonds with the surrounding oxygen atoms, which accumulate more electron density than the sulfur atom. The elevated electron density on the outer oxygen atoms increases donating ability[68] and the *soft* base character of the sulfone. *Soft* bases have a higher affinity to *soft* acids like mercury and silver, and less affinity to *hard* acids like calcium and magnesium, based on the HSAB Pearson acid–base concept.[69] Figure 8 illustrates the potential configuration and interaction of Hg^{2+} with the sulfone group based on earlier work.[70] More details are provided in the SI (Section S9).

CONCLUSIONS

We have designed, synthesized, and structurally characterized a new series of isoreticuar LMOFs containing tppe chromophore ligand and a functionalized coligand. In addition, we have performed a systematic study to investigate, compare, and understand their photoluminescent properties and to assess

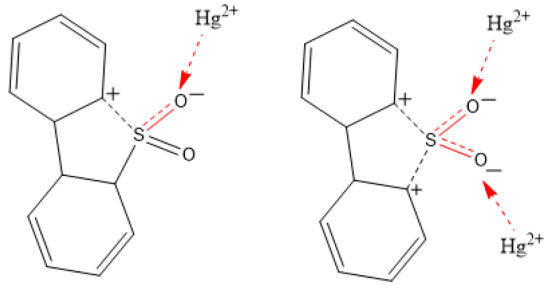

Figure 8. Interaction mechanism of Hg^{2+} with the sulfone functional group.

DOI: 10.1021/acsami.6b10890
ACS Appl. Mater. Interfaces 2016, 8, 30294–30303

their potential as chemical sensors and adsorbents for heavy metals. LMOF-263, specifically, is a porous, water-stable, blue-emitting MOF with a high IQY (89.2%) and a BET surface area of 1004 m^2/g. LMOF-263 acts as a highly sensitive and selective sensor, capable of detecting heavy metal ions in water at very low concentrations (e.g., 3.3 ppb for Hg^{2+} and 19.7 ppb for Pb^{2+}) and has an high Hg^{2+} uptake capacity of ~380 mg/g. The detection ratio for Hg^{2+} compared to light metals Mg^{2+} and Ca^{2+} are 209.5 and 167.4, respectively, illustrating the excellent selectivity of LMOF-263 for heavy metal ions. The achieved K_{SV} values are among the highest in their class for Hg^{2+} (459,446 M^{-1}) and Pb^{2+} (55, 017 M^{-1}). No other MOFs reported to date have had such high performances in both the detection and adsorption of toxic heavy metals. The Hg^{2+} adsorption process follows a fast, pseudo-second-order kinetics model (rate constant: 0.295 g mg^{-1} min^{-1}), removing 99.1% of the total contaminant amount within 30 min. LMOF-263 selectively adsorbed Hg^{2+} when exposed to a mixture of heavy and light metals.

These results suggest that LMOF-263 is well suitable for the simultaneous optical detection (through luminescence quenching) and selective removal of heavy metals (e.g., Hg^{2+}, Pb^{2+}) from aqueous solution. XPS data provide direct evidence for the interaction of Hg^{2+} with the sulfone moeity, underscoring the role of sulfur and oxygen in the LMOF functionality. Materials that have the ability to detect low concentrations and selectively adsorb heavy metals can greatly benefit environmental remediation efforts. Simple and cost-effective optical detection methods using these materials would prove to be valuable for populations across the globe. Our future work will continue on the development and optimization of high-performance LMOFs in solving critical environmental problems.

■ ASSOCIATED CONTENT

Supporting Information

The Supporting Information is available free of charge on the ACS Publications website at DOI: 10.1021/acsami.6b10890.

PXRD, TGA, optical properties, and additional references (PDF)

■ AUTHOR INFORMATION

Corresponding Author

*E-mail: jingli@rutgers.edu (J.L.).

Notes

The authors declare no competing financial interest.

■ ACKNOWLEDGMENTS

We are grateful for the financial support from the Department of Energy, Basic Energy Sciences, Division of Materials Sciences and Engineering through Grant No. DE-FG02-08ER-46491. The Advanced Light Source is supported by the Director, Office of Science, Office of Basic Energy Sciences, of the U.S. Department of Energy under Contract No. DE-AC02-05CH11231. We would also like to thank Horiba Scientific for the loan of the XGT-1000WR EDXRF spectrometer. N.R. would like to especially thank Ben Deibert and Baiyan Li for their extensive and valued discussions.

■ REFERENCES

(1) Hanna-Attisha, M.; LaChance, J.; Sadler, R. C.; Champney Schnepp, A. Elevated Blood Lead Levels in Children Associated With the Flint Drinking Water Crisis: A Spatial Analysis of Risk and Public Health Response. *Am. J. Public Health* **2016**, *106*, 283−290.

(2) Bai, L.; Wang, Y.; Guo, Y.; Zhou, Y.; Xie, Z. Health Risk Assessment Research on Heavy Metals Ingestion Through Groundwater Drinking Pathway for the Residents in Baotou, China. *J. Environ. Health* **2016**, *78*, 84−90.

(3) Xuan, F.; Luo, X.; Hsing, I. M. Conformation-Dependent Exonuclease III Activity Mediated by Metal Ions Reshuffling on Thymine-Rich DNA Duplexes for an Ultrasensitive Electrochemical Method for Hg^{2+} Detection. *Anal. Chem.* **2013**, *85*, 4586−4593.

(4) Jena, B. K.; Raj, C. R. Gold Nanoelectrode Ensembles for the Simultaneous Electrochemical Detection of Ultratrace Arsenic, Mercury, and Copper. *Anal. Chem.* **2008**, *80*, 4836−4844.

(5) Xiao, Y.; Rowe, A. A.; Plaxco, K. W. Electrochemical Detection of Parts-Per-Billion Lead via an Electrode-Bound DNAzyme Assembly. *J. Am. Chem. Soc.* **2007**, *129*, 262−263.

(6) Zhang, Y.; Zeng, G. M.; Tang, L.; Chen, J.; Zhu, Y.; He, X. X.; He, Y. Electrochemical Sensor Based on Electrodeposited Graphene-Au Modified Electrode and NanoAu Carrier Amplified Signal Strategy for Attomolar Mercury Detection. *Anal. Chem.* **2015**, *87*, 989−996.

(7) Zhou, Y.; Dong, H.; Liu, L.; Li, M.; Xiao, K.; Xu, M. Selective and Sensitive Colorimetric Sensor of Mercury(II) Based on Gold Nanoparticles and 4-Mercaptophenylboronic Acid. *Sens. Actuators, B* **2014**, *196*, 106−111.

(8) Maghasi, A. T.; Conklin, S. D.; Shtoyko, T.; Piruska, A.; Richardson, J. N.; Seliskar, C. J.; Heineman, W. R. Spectroelectrochemical Sensing Based on Attenuated Total Internal Reflectance Stripping Voltammetry. 2. Determination of Mercury and Lead. *Anal. Chem.* **2004**, *76*, 1458−1465.

(9) Aragay, G.; Pons, J.; Merkoci, A. Recent Trends in Macro-, Micro-, and Nanomaterial-Based Tools and Strategies for Heavy-Metal Detection. *Chem. Rev.* **2011**, *111*, 3433−3458.

(10) Nolan, E. M.; Lippard, S. J. Tools and Tactics for the Optical Detection of Mercuric Ion. *Chem. Rev.* **2008**, *108*, 3443−3480.

(11) Xie, J.; Zheng, Y.; Ying, J. Y. Highly Selective and Ultrasensitive Detection of $Hg^{(2+)}$ based on Fluorescence Quenching of Au Nanoclusters by $Hg^{(2+)}$-$Au^{(+)}$ Interactions. *Chem. Commun.* **2010**, *46*, 961−963.

(12) Cai, S.; Lao, K.; Lau, C.; Lu, J. "Turn-On" Chemiluminescence Sensor for the Highly Selective and Ultrasensitive Detection of Hg^{2+} Ions Based on Interstrand Cooperative Coordination and Catalytic Formation of Gold Nanoparticles. *Anal. Chem.* **2011**, *83*, 9702−9708.

(13) Chen, B.; Wang, L.; Xiao, Y.; Fronczek, F. R.; Xue, M.; Cui, Y.; Qian, G. A Luminescent Metal-Organic Framework with Lewis Basic Pyridyl Sites for the Sensing of Metal Ions. *Angew. Chem., Int. Ed.* **2009**, *48*, 500−503.

(14) Cui, Y.; Song, R.; Yu, J.; Liu, M.; Wang, Z.; Wu, C.; Yang, Y.; Wang, Z.; Chen, B.; Qian, G. Dual-Emitting MOF Supersetdye Composite for Ratiometric Temperature Sensing. *Adv. Mater.* **2015**, *27*, 1420−1425.

(15) Cui, Y.; Xu, H.; Yue, Y.; Guo, Z.; Yu, J.; Chen, Z.; Gao, J.; Yang, Y.; Qian, G.; Chen, B. A Luminescent Mixed-Lanthanide Metal-Organic Framework Thermometer. *J. Am. Chem. Soc.* **2012**, *134*, 3979−3982.

(16) Cui, Y.; Yue, Y.; Qian, G.; Chen, B. Luminescent Functional Metal-Organic Frameworks. *Chem. Rev.* **2012**, *112*, 1126−1162.

(17) Allendorf, M. D.; Bauer, C. A.; Bhakta, R. K.; Houk, R. J. Luminescent Metal-Organic Frameworks. *Chem. Soc. Rev.* **2009**, *38*, 1330−1352.

(18) Hu, Z.; Deibert, B. J.; Li, J. Luminescent Metal-Organic Frameworks for Chemical Sensing and Explosive Detection. *Chem. Soc. Rev.* **2014**, *43*, 5815−5840.

(19) Perry, J. J., IV; Feng, P. L.; Meek, S. T.; Leong, K.; Doty, F. P.; Allendorf, M. D. Connecting Structure with Function in Metal−Organic Frameworks to Design Novel Photo- and Radioluminescent Materials. *J. Mater. Chem.* **2012**, *22*, 10235−10248.

(20) Bhunia, A.; Esquivel, D.; Dey, S.; Fernández-Terán, R. J.; Goto, Y.; Inagaki, S.; Van Der Voort, P.; Janiak, C. A Photoluminescent Covalent Triazine Framework: CO_2 Adsorption, Light-Driven Hydro-

DOI: 10.1021/acsami.6b10890
ACS Appl. Mater. Interfaces 2016, 8, 30294−30303

gen Evolution and Sensing of Nitroaromatics. *J. Mater. Chem. A* **2016**, *4*, 13450−13457.
(21) Desai, A. V.; Samanta, P.; Manna, B.; Ghosh, S. K. Aqueous Phase Nitric Oxide Detection by an Amine-Decorated Metal-Organic Framework. *Chem. Commun.* **2015**, *51*, 6111−6114.
(22) Joarder, B.; Desai, A. V.; Samanta, P.; Mukherjee, S.; Ghosh, S. K. Selective and Sensitive Aqueous-Phase Detection of 2,4,6-Trinitrophenol (TNP) by an Amine-Functionalized Metal-Organic Framework. *Chem. - Eur. J.* **2015**, *21*, 965−969.
(23) Shahat, A.; Hassan, H. M.; Azzazy, H. M. Optical Metal-Organic Framework Sensor for Selective Discrimination of Some Toxic Metal Ions in Water. *Anal. Chim. Acta* **2013**, *793*, 90−98.
(24) Wu, L. L.; Wang, Z.; Zhao, S. N.; Meng, X.; Song, X. Z.; Feng, J.; Song, S. Y.; Zhang, H. J. A Metal-Organic Framework/DNA Hybrid System as a Novel Fluorescent Biosensor for Mercury(II) Ion Detection. *Chem. - Eur. J.* **2016**, *22*, 477−480.
(25) Liu, B.; Huang, Y.; Zhu, X.; Hao, Y.; Ding, Y.; Wei, W.; Wang, Q.; Qu, P.; Xu, M. Smart Lanthanide Coordination Polymer Fluorescence Probe for Mercury(II) Determination. *Anal. Chim. Acta* **2016**, *912*, 139−145.
(26) Li, L.; Chen, Q.; Niu, Z.; Zhou, X.; Yang, T.; Huang, W. Lanthanide MOFs Assembled from Fluorene-Based Ligand: Selective Sensing of Pb^{2+} and Fe^{3+} Ions. *J. Mater. Chem. C* **2016**, *4*, 1900−1905.
(27) Tan, H.; Liu, B.; Chen, Y. Lanthanide Coordination Polymer Nanoparticles for Sensing of Mercury(II) by Photoinduced Electron Transfer. *ACS Nano* **2012**, *6*, 10505−10511.
(28) Wang, H. M.; Yang, Y. Y.; Zeng, C. H.; Chu, T. S.; Zhu, Y. M.; Ng, S. W. A Highly Luminescent Terbium-Organic Framework for Reversible Detection of Mercury Ions in Aqueous Solution. *Photochem. Photobiol. Sci.* **2013**, *12*, 1700−1706.
(29) Zhu, Y.-M.; Zeng, C.-H.; Chu, T.-S.; Wang, H.-M.; Yang, Y.-Y.; Tong, Y.-X.; Su, C.-Y.; Wong, W.-T. A Novel Highly Luminescent LnMOF Film: A Convenient Sensor for Hg^{2+} Detecting. *J. Mater. Chem. A* **2013**, *1*, 11312−11319.
(30) Xu, H.; Gao, J.; Qian, X.; Wang, J.; He, H.; Cui, Y.; Yang, Y.; Wang, Z.; Qian, G. Metal−Organic Framework Nanosheets for Fast-Response and Highly Sensitive Luminescent Sensing of Fe^{3+}. *J. Mater. Chem. A* **2016**, *4*, 10900−10905.
(31) Ke, F.; Qiu, L. G.; Yuan, Y. P.; Peng, F. M.; Jiang, X.; Xie, A. J.; Shen, Y. H.; Zhu, J. F. Thiol-Functionalization of Metal-Organic Framework by a Facile Coordination-Based Postsynthetic Strategy and Enhanced Removal of Hg^{2+} from Water. *J. Hazard. Mater.* **2011**, *196*, 36−43.
(32) Saleem, H.; Rafique, U.; Davies, R. P. Investigations on Post-Synthetically Modified UiO-66-NH_2 for the Adsorptive Removal of Heavy Metal Ions from Aqueous Solution. *Microporous Mesoporous Mater.* **2016**, *221*, 238−244.
(33) Yee, K. K.; Reimer, N.; Liu, J.; Cheng, S. Y.; Yiu, S. M.; Weber, J.; Stock, N.; Xu, Z. Effective Mercury Sorption by Thiol-Laced Metal-Organic Frameworks: In Strong Acid and the Vapor Phase. *J. Am. Chem. Soc.* **2013**, *135*, 7795−7798.
(34) Xu, X.-Y.; Yan, B. Fabrication and Application of a Ratiometric and Colorimetric Fluorescent Probe for Hg^{2+} Based on Dual-Emissive Metal-Organic Framework Hybrids with Carbon Dots and Eu^{3+}. *J. Mater. Chem. C* **2016**, *4*, 1543−1549.
(35) Li, B.; Zhang, Y.; Ma, D.; Shi, Z.; Ma, S. Mercury Nano-Trap for Effective and Efficient Removal of Mercury(II) from Aqueous Solution. *Nat. Commun.* **2014**, *5*, 5537.
(36) Nagarkar, S. S.; Joarder, B.; Chaudhari, A. K.; Mukherjee, S.; Ghosh, S. K. Highly Selective Detection of Nitro Explosives by a Luminescent Metal-Organic Framework. *Angew. Chem., Int. Ed.* **2013**, *52*, 2881−2885.
(37) Hu, Z.; Tan, K.; Lustig, W. P.; Wang, H.; Zhao, Y.; Zheng, C.; Banerjee, D.; Emge, T. J.; Chabal, Y. J.; Li, J. Effective Sensing of RDX via Instant and Selective Detection of Ketone Vapors. *Chem. Sci.* **2014**, *5*, 4873−4877.
(38) Sanda, S.; Parshamoni, S.; Biswas, S.; Konar, S. Highly Selective Detection of Palladium and Picric Acid by a Luminescent MOF: A Dual Functional Fluorescent Sensor. *Chem. Commun.* **2015**, *51*, 6576−6579.
(39) Gong, Q.; Hu, Z.; Deibert, B. J.; Emge, T. J.; Teat, S. J.; Banerjee, D.; Mussman, B.; Rudd, N. D.; Li, J. Solution Processable MOF Yellow Phosphor with Exceptionally High Quantum Efficiency. *J. Am. Chem. Soc.* **2014**, *136*, 16724−16727.
(40) Hu, Z.; Lustig, W. P.; Zhang, J.; Zheng, C.; Wang, H.; Teat, S. J.; Gong, Q.; Rudd, N. D.; Li, J. Effective Detection of Mycotoxins by a Highly Luminescent Metal-Organic Framework. *J. Am. Chem. Soc.* **2015**, *137*, 16209−16215.
(41) Hu, Z.; Huang, G.; Lustig, W. P.; Wang, F.; Wang, H.; Teat, S. J.; Banerjee, D.; Zhang, D.; Li, J. Achieving Exceptionally High Luminescence Quantum Efficiency by Immobilizing an AIE Molecular Chromophore into a Metal-Organic Framework. *Chem. Commun.* **2015**, *51*, 3045−3048.
(42) Li, B.; Chrzanowski, M.; Zhang, Y.; Ma, S. Applications of Metal-Organic Frameworks Featuring Multi-Functional Sites. *Coord. Chem. Rev.* **2016**, *307*, 106−129.
(43) Eddaoudi, M.; Kim, J.; Rosi, N.; Vodak, D.; Wachter, J.; O'Keeffe, M.; Yaghi, O. M. Systematic Design of Pore Size and Functionality in Isoreticular MOFs and Their Application in Methane Storage. *Science* **2002**, *295*, 469−472.
(44) Ol'kohovik, V.; Vasilevskii, D.; Pap, A.; Kalechyts, G.; Matveienko, Y.; Baran, A.; Halinouski, N.; Petushok, V. Synthesis of New Polyconjugated Molecules with Biphenyl, Dibenzothiophene, Carbazole and Phenanthrene Units. *Arkivoc* **2008**, *9*, 69−93.
(45) Ding, S. Y.; Dong, M.; Wang, Y. W.; Chen, Y. T.; Wang, H. Z.; Su, C. Y.; Wang, W. Thioether-Based Fluorescent Covalent Organic Framework for Selective Detection and Facile Removal of Mercury-(II). *J. Am. Chem. Soc.* **2016**, *138*, 3031−3037.
(46) Wu, P.; Liu, Y.; Wang, J.; Li, Y.; Liu, W. Cadmium-Based Metal-Organic Framework as a Highly Selective and Sensitive Ratiometric Luminescent Sensor for Mercury(II). *Inorg. Chem.* **2015**, *54*, 11046−11048.
(47) Wen, L.; Zheng, X.; Lv, K.; Wang, C.; Xu, X. Two Amino-Decorated Metal-Organic Frameworks for Highly Selective and Quantitatively Sensing of Hg(II) and Cr(VI) in Aqueous Solution. *Inorg. Chem.* **2015**, *54*, 7133−7135.
(48) Shan, F.-S.; Lai, J.-P.; Sun, H.; Zhang, P.; Luo, C.; He, Y.-H.; Feng, H.-R. A Facile, Fast Responsive and Highly Selective Mercury (II) Probe: Characterized by the Fluorescence Quenching of 2,9-Dimethyl-1,10-Phenanthroline and Two New Metal-Organic Frameworks. *RSC Adv.* **2016**, *6*, 66215−66223.
(49) Xu, F.; Kou, L.; Jia, J.; Hou, X.; Long, Z.; Wang, S. Metal-Organic Frameworks of Zeolitic Imidazolate Framework-7 and Zeolitic Imidazolate Framework-60 for Fast Mercury and Methylmercury Speciation Analysis. *Anal. Chim. Acta* **2013**, *804*, 240−245.
(50) Yang, J.; Wang, Z.; Li, Y.; Zhuang, Q.; Zhao, W.; Gu, J. Porphyrinic MOFs for Reversible Fluorescent and Colorimetric Sensing of Mercury(II) Ions in Aqueous-Phase. *RSC Adv.* **2016**, *6*, 69807−69814.
(51) Lu, W.; Qin, X.; Liu, S.; Chang, G.; Zhang, Y.; Luo, Y.; Asiri, A. M.; Al-Youbi, A. O.; Sun, X. Economical, Green Synthesis of Fluorescent Carbon Nanoparticles and Their Use as Probes for Sensitive and Selective Detection Of Mercury(II) Ions. *Anal. Chem.* **2012**, *84*, 5351−5357.
(52) Jurado-Sánchez, B.; Escarpa, A.; Wang, J. Lighting Up Micromotors with Quantum Dots for Smart Chemical Sensing. *Chem. Commun.* **2015**, *51*, 14088−14091.
(53) Zhou, Y.; Chen, H.-H.; Yan, B. An Eu^{3+} Post-Functionalized Nanosized Metal−Organic Framework for Cation Exchange-Based Fe^{3+}-Sensing In An Aqueous Environment. *J. Mater. Chem. A* **2014**, *2*, 13691−13697.
(54) Yang, C. X.; Ren, H. B.; Yan, X. P. Fluorescent Metal-Organic Framework MIL-53(Al) for Highly Selective and Sensitive Detection of Fe^{3+} in Aqueous Solution. *Anal. Chem.* **2013**, *85*, 7441−7446.
(55) Yantasee, W.; Rutledge, R. D.; Chouyyok, W.; Sukwarotwat, V.; Orr, G.; Warner, C. L.; Warner, M. G.; Fryxell, G. E.; Wiacek, R. J.; Timchalk, C.; Addleman, R. S. Functionalized Nanoporous Silica for

DOI: 10.1021/acsami.6b10890
ACS Appl. Mater. Interfaces 2016, 8, 30294−30303

the Removal of Heavy Metals from Biological Systems: Adsorption and Application. *ACS Appl. Mater. Interfaces* **2010**, *2*, 2749−2758.
(56) Shin, Y.; Fryxell, G. E.; Um, W.; Parker, K.; Mattigod, S. V.; Skaggs, R. Sulfur-Functionalized Mesoporous Carbon. *Adv. Funct. Mater.* **2007**, *17*, 2897−2901.
(57) Manos, M. J.; Petkov, V. G.; Kanatzidis, M. G. $H_{2x}Mn_xSn_{3-x}S_6$ (x = 0.11−0.25): A Novel Reusable Sorbent for Highly Specific Mercury Capture Under Extreme pH Conditions. *Adv. Funct. Mater.* **2009**, *19*, 1087−1092.
(58) Mon, M.; Ferrando-Soria, J.; Grancha, T.; Fortea-Perez, F. R.; Gascon, J.; Leyva-Perez, A.; Armentano, D.; Pardo, E. Selective Gold Recovery and Catalysis in a Highly Flexible Methionine-Decorated Metal-Organic Framework. *J. Am. Chem. Soc.* **2016**, *138*, 7864−7867.
(59) Luo, F.; Chen, J. L.; Dang, L. L.; Zhou, W. N.; Lin, H. L.; Li, J. Q.; Liu, S. J.; Luo, M. B.; Luo, M. B. High Performance Hg(II) Removal from Low Concentration Aqueous Solutions Using Acylamide and Hydroxyl MOFs. *J. Mater. Chem. A* **2015**, *3*, 9616−9620.
(60) He, J.; Yee, K.-K.; Xu, Z.; Zeller, M.; Hunter, A. D.; Chui, S. S.-Y.; Che, C.-M. Thioether Side Chains Improve the Stability, Fluorescence, and Metal Uptake of a Metal−Organic Framework. *Chem. Mater.* **2011**, *23*, 2940−2947.
(61) Huang, L.; He, M.; Chen, B.; Hu, B. A Mercapto-Functionalized Magnetic Zr-MOF by Solvent-Assisted Ligand Exchange for Hg^{2+} Removal from Water. *J. Mater. Chem. A* **2016**, *4*, 5159−5166.
(62) Luo, X.; Shen, T.; Ding, L.; Zhong, W.; Luo, J.; Luo, S. Novel Thymine-Functionalized MIL-101 Prepared by Post-Synthesis and Enhanced Removal of $Hg^{(2+)}$ from Water. *J. Hazard. Mater.* **2016**, *306*, 313−322.
(63) Wu, Y.; Xu, G.; Liu, W.; Yang, J.; Wei, F.; Li, L.; Zhang, W.; Hu, Q. Postsynthetic Modification of Copper Terephthalate Metal-Organic Frameworks and Their New Application in Preparation of Samples Containing Heavy Metal Ions. *Microporous Mesoporous Mater.* **2015**, *210*, 110−115.
(64) Wang, K.; Huang, H.; Xue, W.; Liu, D.; Zhao, X.; Xiao, Y.; Li, Z.; Yang, Q.; Wang, L.; Zhong, C. An Ultrastable Zr Metal−Organic Framework with a Thiophene-Type Ligand Containing Methyl Groups. *CrystEngComm* **2015**, *17*, 3586−3590.
(65) Chakraborty, A.; Bhattacharyya, S.; Hazra, A.; Ghosh, A. C.; Maji, T. K. Post-Synthetic Metalation in an Anionic MOF for Efficient Catalytic Activity and Removal of Heavy Metal Ions from Aqueous Solution. *Chem. Commun.* **2016**, *52*, 2831−2834.
(66) Huang, L.; He, M.; Chen, B.; Hu, B. A Designable Magnetic MOF Composite and Facile Coordination-Based Post-Synthetic Strategy for the Enhanced Removal of Hg^{2+} from Water. *J. Mater. Chem. A* **2015**, *3*, 11587−11595.
(67) Fang, Q. R.; Yuan, D. Q.; Sculley, J.; Li, J. R.; Han, Z. B.; Zhou, H. C. Functional Mesoporous Metal-Organic Frameworks for the Capture of Heavy Metal Ions and Size-Selective Catalysis. *Inorg. Chem.* **2010**, *49*, 11637−11642.
(68) Drago, R. S.; Wayland, B.; Carlson, R. L. Donor Properties of Sulfoxides, Alkyl Sulfites, and Sulfones. *J. Am. Chem. Soc.* **1963**, *85*, 3125−3128.
(69) Block, E. *Reactions of Organosulfur Compounds: Organic Chemistry: A Series of Monographs*; Academic Press: Cambridge, 2013; Vol. *37*.
(70) Niu, Y.; Zhao, S.; Chen, G.; Qu, R.; Zhou, C.; Wang, L.; Feng, S. Combined Theoretical and Experimental Study on the Adsorption Mechanism of Poly(4-vinylbenzyl-2-hydroxyethyl)sulfide, Sulfoxide, and Sulfone for Hg(II) and Pb(II). *J. Mol. Liq.* **2016**, *219*, 1065−1070.

DOI: 10.1021/acsami.6b10890
ACS Appl. Mater. Interfaces 2016, 8, 30294−30303